Topological centrality-based identification of hub genes and pathways associated with acute viral respiratory infection in infants

X.Y. Liu[1], G.Q. Li[2], Y. Ma[3] and L.J. Zhao[4]

[1]Department of Test Cabinet, The Third Hospital of Jinan, Jinan, China
[2]Department of Pediatrics, The Third Hospital of Jinan, Jinan, China
[3]Department of Out-patient, The Third Hospital of Jinan, Jinan, China
[4]Department of Pediatrics, Shandong Provincial Hospital, Shandong, China

Corresponding author: L.J. Zhao
E-mail: lijianzhao2015@yeah.net

Genet. Mol. Res. 14 (4): 18334-18343 (2015)
Received August 10, 2015
Accepted September 29, 2015
Published December 23, 2015
DOI http://dx.doi.org/10.4238/2015.December.23.21

ABSTRACT. The objective of this study was to identify hub genes and pathways associated with acute respiratory infection (ARI) in infants based on gene expression profiles. Differentially expressed genes (DEGs) between ARI and normal (controls) infants were identified based on linear modeling of the microarray data using Limma package. A protein-protein interaction (PPI) network was constructed using the Search Tool for the Retrieval of Interacting Genes/proteins and clusters were obtained by employing the molecular complex detection algorithm. Topological centrality was applied to characterize the biological importance of genes in the network. Functional enrichment analysis of the genes was performed based on the expression analysis systematic explore test. In total, 116 DEGs between ARI and controls were identified. Of the 61 nodes and 189 edges in the PPI network generated with the DEGs, three clusters were mined. Six hub genes namely *RPL6*, *RPL3*, *EEF1B2*, *RPL15*, *EEF1A1*, and *RPS2*, which were identified based on the topological centrality measures, were evaluated further. Functional enrichment analysis revealed that DEGs were

significantly enriched in terms of Gene Ontology translational elongation, structural constituent of ribosome, and cytosol. The most significant term of pathway analysis was “ribosome”. In summary, this study suggests *RPL6*, *RPL3*, and *RPL15* as hub genes and the ribosome pathway to be significantly associated with viral ARI in infants, which might also be used as potential markers for the viral etiology.

Key words: Acute respiratory infection; Hub genes; Ribosome pathway; Protein-protein interaction network

INTRODUCTION

Acute respiratory infection (ARI) is a leading killer of children and responsible for at least six percent of the world’s disability and death (Lyczkowski et al., 2014). Respiratory syncytial virus (RSV), rhinovirus (HRV) and influenza A (Flu A) are among the most commonly implicated etiological agents of ARI A) (Chang et al., 2010; Huang et al., 2013).

Several studies on the viral etiology and clinical characteristics of ARI have been published in recent years (Zaas et al., 2009; Kamban and Svavarsdottir, 2013). Zaas et al. (2009) developed gene expression signatures from peripheral blood samples, which distinguished individuals with symptomatic ARI from uninfected individuals and viral from bacterial ARI. Although, the most up-regulated (*IFI27*) and down-regulated (*CLC*) genes in the whole blood of infants hospitalized with RSV subtype B and bronchiolitis are known (Fjaerli et al., 2006), detection and treatment of viral infection is still limited due to lack of diagnostic markers and clinical studies respectively (Hirsch et al., 2013). Therefore, it is critical to discover the pathogenesis and prevent further ARI infections in infants and related complications.

In this paper, firstly, differentially expressed genes (DEGs) between ARI and normal controls were identified using linear modeling of gene expression data. Subsequently, a protein-protein interaction (PPI) network was constructed based on DEGs using the Search Tool for the Retrieval of Interacting Genes/proteins (STRING) and clusters were obtained by employing the Molecular Complex Detection (MCODE) algorithm. Further, topological centrality (degree, stress, closeness, and betweenness) analysis for networks was employed to identify hub genes. Finally, functional enrichment analysis of DEGs and hub genes performed according to the expression analysis systematic explore (EASE) test revealed the pathway potentially related to ARI in infants.

MATERIAL AND METHODS

Data collection and preprocessing

The microarray gene expression profile of RSV infected infants (accession number: GSE38900), which was obtained using the Illumina HumanWG-6 v3 platform 900(Mejias et al., 2013) was extracted from National Center for Biotechnology Information’s (NCBI) Gene Expression Omnibus. Samples of GSE38900 were divided into four groups namely RSV (107 patients), HRV (30 patients), Flu A (36 patients), and control (27 subjects).

The quality of gene microarray probe-level data of GSE38900 was controlled by standard procedures in four steps, background correction (Irizarry et al., 2003), normalization (Bolstad et al., 2003), probe correction (Bolstad, 2013) and summarization (Irizarry et al., 2003). In brief,

background correction and normalization were performed by applying the Robust Multi-array Average (RMA) algorithm and a quantile function-based algorithm to eliminate the influence of non-specific hybridization. Perfect match and mismatch were revised by utilizing the Micro Array Suite (MAS) algorithm. Lastly, gene expression values were summarized according to the median polish technique. The pre-processed probe-level dataset in CEL format was converted into expression measures and screened by feature filter function of genefilter package (Lee and Kim, 2012).

Identification of differentially expressed genes (DEGs)

In this paper, DEGs between ARI in infants and controls were identified using the Limma package (Smyth, 2004). All genes were subjected to *t*-test and *F*-test followed by linear model fitting, empirical Bayes statistics for differential expression and correction for false discovery rate (FDR) were performed by using lmFit function (Diboun et al., 2006). DEGs identified with a threshold of $P < 0.05$ and $|\log_2 FC| > 2$ were analyzed further. Each of the three groups of DEGs (RSV, HRV, and Flu A) was compared to the other two as well as the control group, respectively. The common DEGs upon combining the three groups (intersection) are referred as DEGs henceforth.

Construction of PPI network and identification of clusters

For protein interaction data, we utilized aNG. A PPI network was constructed using the DEGs based on a human PPI dataset from the STRING in Cytoscape (Smoot et al., 2011), a free software package for visualizing, modeling, and analyzing the integration of biomolecular interaction networks from high-throughput expression data and other molecular states. In PPI networks, a node stands for the gene and edge stands for the interaction of genes.

MCODE algorithm that recognizes specific functional modules in a network by selecting clusters with densely connected nodes was employed for extracting significant sub-networks from the PPI network (Spinelli et al., 2013). It mainly included three stages namely vertex weighting, complex prediction, and post-processing. Sub-networks that met the following threshold values (node score cutoff = 0.2, degree cutoff = 4, K-core = 4, Max. depth = 100) were detected as clusters for DEGs.

Topological centrality analysis

In PPI network analysis, it is fundamental to determine the importance of a particular node, quantifying centrality and connectivity in order to identify portions that may play interesting roles (Bader and Madduri, 2006). In the present paper, the biological importance of genes in the PPI network was characterized using indices of topological centrality, both at local scale (degree) and global scale (stress centrality, closeness centrality and betweenness centrality) (Wasserman, 1994; Haythornthwaite, 1996; Barthelemy, 2004; Fekete et al., 2005). In addition, genes with ≥90% degree quantile distribution in the network of significant DEGs were defined as hub genes.

Degree centrality

Degree quantifies the local topology of each gene, by summing up the number of its adjacent genes (Wasserman, 1994). It gives a simple count of the number of interactions of a given node. The degree $C_D(v)$ of a node v is defined as:

$$C_D(v) = \sum_j a_{vj} \quad \text{(Equation 1)}$$

Stress centrality

Stress centrality is the number of nodes in the shortest path between two nodes (Fekete et al., 2005). To calculate the stress $C_{str}(v)$ of a node v, all shortest paths in a graph G are calculated and then the number of shortest paths passing through v counted. A "stressed" node is a node traversed by a high number of shortest paths. σst is the total number of shortest paths from node s to node t and $\sigma st\ (v)$ is the number of those paths that pass through v. $C_{str}(v)$ is calculated as follows:

$$C_{str}(v) = \sum_{s \neq v \in N} \sum_{t \neq v \in N} \sigma_{st}(v) \quad \text{(Equation 2)}$$

Closeness centrality

Closeness centrality is the measure of the average length of the shortest paths to access all other proteins in the network (Barthelemy, 2004). The larger the value, the more central is the protein. The closeness centrality, $C_c(v)$ was calculated for every functional category by considering all the shortest paths for each node. $C_c(v)$ of node v is defined as the reciprocal of the average shortest path length and is computed as follows:

$$C_C(v) = \frac{1}{\sum_{t \in N} d_G(v,t)} \quad \text{(Equation 3)}$$

where $dG(v, t)$ represents the length of the shortest path between two nodes v and t in graph G, which is the sum of the weights of all edges on this shortest path. Meanwhile, $dG(v, v) = 0$, $dG(v, t) = dG(t, v)$ in undirected graph.

Betweenness centrality

Betweenness centrality is another topological metric in graphs for determining how the neighbors of a node are interconnected (Haythornthwaite, 1996). It is the ratio of the node in the shortest path between two other nodes. The betweenness centrality of a node v is given by the expression:

$$C_B(v) = \sum_{s \neq v \neq t \in N} \frac{\sigma_{st(v)}}{\sigma_{st}} \quad \text{(Equation 4)}$$

Betweenness centrality of a node scales with the number of pairs of nodes as implied by the summation indices. Therefore, the calculation may be rescaled by dividing the number of pairs of nodes not including v, so $C_B(v) \in [0,1]$.

Functional enrichment analysis

Further to investigate the biological functions, Gene Ontology (GO) and KEGG pathway

enrichment from the Database for Annotation, Visualization, and Integrated Discovery (DAVID) were performed (Huang et al., 2008). GO terms and KEGG pathways with P value < 0.05 were selected based on EASE test implemented in DAVID. EASE analysis of the regulated genes revealed molecular functions and biological processes unique to each category (Ford et al., 2006). The EASE score was used as a measure of significance of the categories. In both the functional and pathway enrichment analysis, the minimum threshold of >2 genes for the corresponding term was considered significant for a category. P value was calculated using the formula

$$P = \frac{\binom{a+b}{a}\binom{c+d}{c}}{\binom{n}{a+c}} \quad \text{(Equation 5)}$$

in which, $n = a' + b + c + d$ was the number of background genes, a' - the gene number of one gene set in the gene lists, and a' was replaced with $a = a'$-1. $a' + b$ was the number of genes in the gene list including at least one gene set; $a' + c$ was the gene number of one gene list in the background genes.

RESULTS

Identification of DEGs

In this study, 973, 1501, and 1177 DEGs were obtained from RSV, HRV, and Flu A groups, respectively. The final list of 116 common DEGs between infants ARI and normal controls was decided following the intersection of the three groups and evaluated.

Construction of PPI network and clusters

In the PPI network, nodes refer to DEGs and edges between nodes indicate the interactions of genes in the network. In the present study, PPI network for ARI in infants based on the 116 DEGs is presented in Figure 1. The 61 DEGs mapped to the network had 189 interactions or edges.

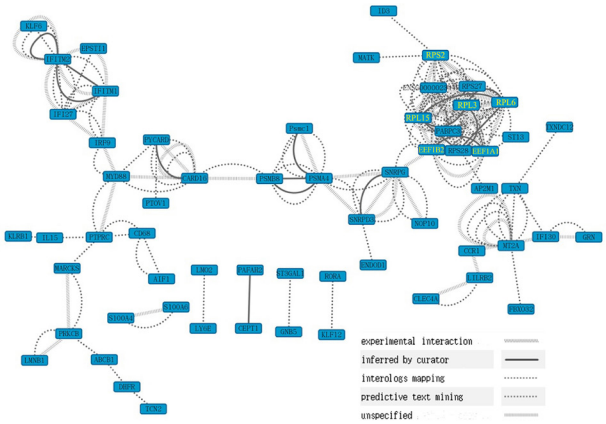

Figure 1. PPI network for ARI in infants based on DEGs. Nodes represent genes, yellow font indicates hub genes, and edges indicate the interactions between genes.

MCODE plugin of the Cytoscape software was used to mine clusters from the PPI network by applying threshold values: Degree Cutoff = 2, K-core = 3, Max. depth = 100, which revealed a total of 3 clusters as shown in Figure 2. The number of genes in Clusters 1, 2 and 3 were 8, 6 and 7 respectively.

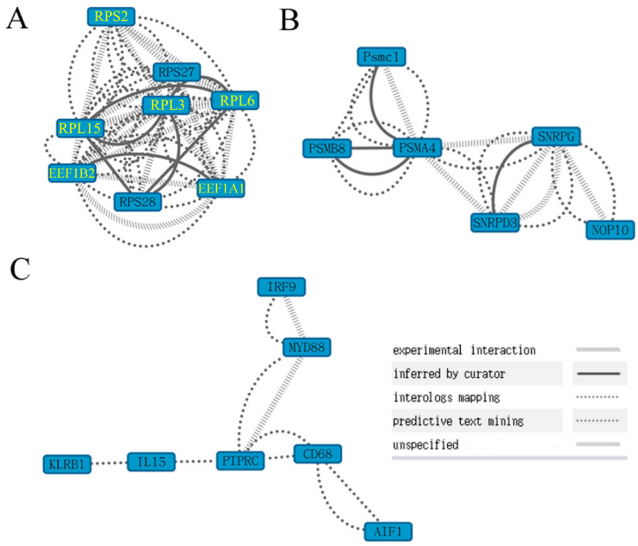

Figure 2. Clusters of PPI network identified by MCODE algorithm. **A.** Cluster 1, **B.** Cluster 2, and **C.** Cluster 3. Nodes represent genes, yellow font indicates hub genes, and edges indicate the interactions between genes.

Topological centrality analysis

Further, to ascertain the significant nodes, topological centrality indices of degree, stress, closeness, and betweenness were calculated for nodes in the PPI network. The results (top 10% listed in Table 1) showed that not all the centrality measures were consistent; however, an overlapping trend between two methods might exist. For example, *EEF1B2* was selected based on degree and stress centralities, whereas *PSMA4*, *MYD88*, *PSMB8*, and *CARD16* were detected according to stress and betweenness centralities. In general, degree centrality was more common and reliable than other types of centralities. Therefore, genes with degrees >15 (top 10% of degree) were described as hub genes. Among the nodes, *RPL6* showed the highest degree (25), followed by *RPL3*, *EEF1B2*, *RPL15*, EEF1A1, and *RPS2* with 24, 21, 21, 17, and 16 degrees in the network, respectively. Because of their higher connectivity, hub genes are believed to possess important biological functions during disease progression. Interestingly, all the hub genes of PPI network were involved in Cluster 1, which indicated the significance of this cluster in ARI in infants.

Functional enrichment analysis

The GO enrichment analysis results showed that the 116 genes were significantly enriched in 9 biological processes (BP) with P-value < 0.05 (Figure 3). In Figure 3, the colored circles represent significant pathways and the arrows indicate the progression of BP terms. The most significant terms were translational elongate (P = 2.67E-11), translation (P = 4.62E-09), and cellular protein metabolic process (P = 1.81E-05). Genes *EEF1A1*, *RPS27*, *RPS28*, *EEF1B2*, *RPL13A*,

RPL6, *RPL15*, *RPL3*, *EEF1G*, *RPL23A*, and *RPS2* were enriched under the term translational elongate. This included all the hub genes, which were also involved in other BP terms such as translation, cellular protein metabolic process, protein metabolic process, gene expression, and cellular macromolecule metabolic process.

In the pathway enrichment analysis, only the ribosome pathway was significantly enriched (P = 4.72E-06) with 8 counts (*RPS27*, *RPS28*, *RPL13A*, *RPL6*, *RPL15*, *RPL3*, *RPL23A* and *RPS2*). Of the 6 hub genes, 4 were ribosomal.

Table 1. Top 10% ranked genes in the PPI network based on centrality analyses.

No.	Degree		Stress		Closeness		Betweenness	
	Terms	Value	Terms	Value	Terms	Value	Terms	Value
1	*RPL6*	25	*SNRPG*	1970	*IFI30*	0.533	*IFI30*	0.679
2	*RPL3*	24	*EEF1B2*	1924	*TXN*	0.500	*TXN*	0.607
3	*EEF1B2*	21	*PSMA4*	1850	*CCR1*	0.444	*MYD88*	0.578
4	*RPL15*	21	*MYD88*	1810	*MT2A*	0.381	*CARD16*	0.512
5	*EEF1A1*	17	*PSMB8*	1794	*GRN*	0.364	*PSMB8*	0.512
6	*RPS2*	16	*CARD16*	1970	*LILRB2*	0.348	*PSMA4*	0.505

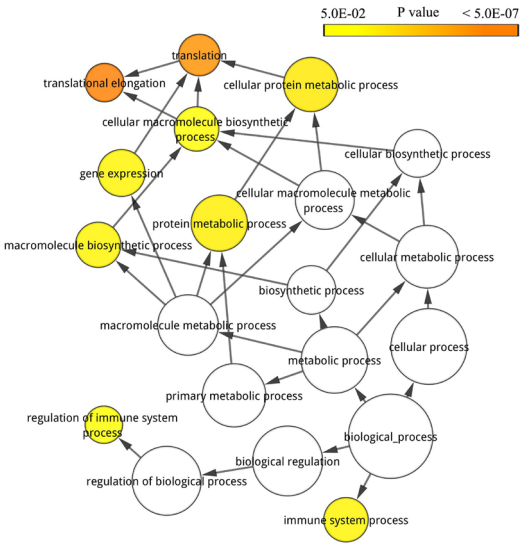

Figure 3. GO enrichment analysis results. Each circle represents a BP term. Colored circles represent significant pathways (P < 0.05) and the arrows indicate progression of BP terms.

DISCUSSION

Previously, Meijas et al. (2013) have presented the gene expression profile of whole blood from infants infected with RSV specifically compared to HRV, Flu A, and normal subjects. In the present study, the significant differentially expressed genes in infants infected by ARI along with their associated sub-networks and signal pathways were added. Furthermore, 6 hub genes (*RPL6*, *RPL3*, *EEF1B2*, *RPL15*, *EEF1A1*, and *RPS2*) and ribosome pathway were identified to be highly relevant to the viral etiology.

Ribosomes, the organelles that catalyze protein synthesis, consist of a small 40S subunit and a large 60S subunit. Together these subunits are composed of 4 RNA species and approximately 80 structurally distinct proteins. *RPL6*, *RPL3*, *RPL15*, and *RPS2* belong to the ribosome protein family. *RPL6* is mapped to chromosome 12q24.1 between the markers D12S84 and D12S861. High expression of *RPL6* was observed in many cancers (Provost et al., 2013) and associated with enhanced resistance to multiple anti-cancer drugs such as adriamycin, vincristine, etoposide, 5-fluorouracil, and cisplatin (Du et al., 2005). Besides, *RPL6* was essential for p53 stabilization (Bai et al., 2013). Our results suggest a strong correlation between ARI in infants the biological processes/pathway in which *RPL6* is involved in.

RPL3 induces G_1/S arrest or apoptosis by modulating p21 (waf1/cip1) levels in a p53-independent manner (Russo et al., 2013). It was shown that *RPL3* over-expression caused an increase in its aberrantly spliced mRNA, which was degraded by the nonsense-mediated decay pathway (Malygin et al., 2007). Moreover, *RPL3* might play an important role in silencing the human embryonic epsilon-globin gene expression (Huang et al., 2000), and its over-expression led to growth inhibition (Eid et al., 2013). Strong down-regulation of the steady state mRNA level of *RPL3* was observed upon induction of differentiation in HL-60 cells (Mailhammer et al., 1992).

RPS2 as is a well-conserved protein of the eukaryotic small ribosomal subunit (Lipson et al., 2010). It localizes in the nucleoplasm and cytoplasm, but is excluded from the nucleoli (Antoine et al., 2005). siRNA treatment (nat-siRNAATGB2) could confer RPS2-mediated cognate host disease resistance by repressing PPRL, which is a putative negative regulator of the *RPS2* resistance pathway (Katiyar-Agarwal et al., 2006).

EEF1B2 encodes an isoform of the alpha subunit of the elongation factor-1 complex, which is responsible for the enzymatic delivery of aminoacyl mRNAs to the ribosome (Wang et al., 2004). *RPL15* (ribosomal protein L15) encodes a ribosomal protein, which is located in the cytoplasm. *EEF1A1* binds defective polypeptides that are released from ribosomes aiding aggresome formation (Meriin et al., 2012).

All theHhub genes *RPL6*, *RPL3*, *RPS2*, *RPS27*, *RPL15*, *EEF1B2*, and *EEF1A1* identified from the PPI network ars related to ribosomal proteins. Furthermore, several BP terms were also associateddwith ribosomal processes. It is well-known that viruses depend on ribosomes to synthesize proteins. Several ribosomal genes or proteins have been indicated to have significant association with virus-related respiratory infectioVs (Ahmadian et al., 2000; Mazumder et al., 2014). The hub genes and the differential expression of ribosomal protein were strongly involved in ARI.

In summary, the hub genes and ribosomal pathway identifiee in this study might be potential biomarkers for the early detection and confirmation of viral etiology of ARI in infants. However, further validatiod and in-depth studies are required to elucidate the interaction between ARI and the hub genes.

Conflicts of interest

The authors declare no conflict of interest.

REFERENCES

Ahmadian G, Randhawa JS and Easton AJ (2000). Expression of the ORF-2 protein of the human respiratory syncytial virus M2 gene is initiated by a rebosomal termination-dependent reinitiation mechanism. *EMBO J.* 1: 2681-2689.

Antoine M, Reimers K, Wirz W, Gressner A, et al. (2005). Identification of an unconventional nuclear localization signal in human ribosomal protein S2. *Biochem. biophys. resh. comm.* 33: 146-153.

Bader DA and Madduri K (2006). Parallel algorithms for evaluating centrality indices in real-world networks. International Conference on Parallel Processin. ICPP, Los Alamitos, 539-550.

Bai D, Zhang J, Xiao W and Zheng X (2013). Regulation of the HDM2-p53 pathway by ribosomal protein L6 in response to ribosomal stress. *Nucleic Acids Res*. 42: 1799-1811.

Barthelemy M (2004). Betweenness centrality in large complex networks. *Eur. Phys. J. B-Condensd Matter Complex Systs* 3: 163-168.

Bolstad B (2013). affy: Built-in Processing Methods. Available at [http://www.bioconductor.org].

Bolstad BM, Irizarry RA, Astrand M and Speed TP (2003). A comparison of normalization methods for high density oligonucleotide array data based on variance and bias. *Bioinformatics* 1: 185-193.

Chang J, Li CY, Li HJ, Luo YC, et al. (2010). Viral etiology of acute respiratory infection in children from Wenzhou between 2007 and 200. *Chin. J. Contemp. Pediatr.* 1: 32-34.

Diboun I, Wernisch L, Orengo CA and Koltzenburg M (2006). Microarray analysis after RNA amplification can detect pronounced differences in gene expression using limma. *BMC Genomics* 7: 252.

Du J, Shi Y, Pan Y, Jin X, et al. (2005). Regulation of multidrug resistance by ribosomal protein l6 in gastric cancer cells. *Cancer Biol. Ther.* 4: 242-247.

Eid R, Sheibani S, Gharib N, Lapointe JF, et al. (2013). Human ribosomal protein L9 is a Bax suppressor that promotes cell survival in yeast. *FEMS Yeast Rec*. 14: 495-507.

Fekete SP, Kaufmann M, Kröller A and Lehmann K (2005). A new approach for boundary recognition in geometric sensor networks. Proceedings 17th Canadian Conference on Computational Geometry, 82-85.

Fjaerli H-O, Bukholm G, Krog A, Skjaeret C, et al. (2006). Whole blood gene expression in infants with respiratory syncytial virus bronchiolitis. *BMC Infect. Dis.* 6: 175.

Ford G, Xu Z, Gates A, Jiang J, et al. (2006). Expression Analysis Systematic Explorer (EASE) analysis reveals differential gene expression in permanent and transient focal stroke rat models. *Brain Res.* 107: 226-236.

Haythornthwaite C (1996). Social network analysis: An approach and technique for the study of information exchange. *Libr. Inf. Sci. Res.* 1: 323-342.

Hirsch HH, Martino R, Ward KN, Boeckh M, et al. (2013). Fourth European Conference on Infections in Leukaemia (ECIL-4): Guidelines for Diagnosis and Treatment of Human Respiratory Syncytial Virus, Parainfluenza Virus, Metapneumovirus, Rhinovirus, and Coronavirus. *Clin. Infect. Dis.* 5: 258-266.

Huang DW, Sherman BT and Lempicki RA (2008). Systematic and integrative analysis of large gene lists using DAVID bioinformatics resources. *Nat. Protoc.* 4: 44-57.

Huang G, Yu D, Mao N, Zhu Z, et al. (2013). Viral Etiology of Acute Respiratory Infection in Gansu Province, China, 2011. *PLoS One* 8: e64254.

Huang J, Hou C and Qian R (2000). Screening of genes related to the expression of human epsilon-globin gene by using yeast one-hybrid system. *Acta Biochima Biophysa Sina* 3: 246-250.

Irizarry RA, Bolstad BM, Collin F, Cope LM, et al. (2003). Summaries of Affymetrix GeneChip probe level data. *Nucleic Acids Res.* 3: e15.

Kamban SW and Svavarsdottir EK (2013). Does a therapeutic conversation intervention in an acute paediatric setting make a difference for families of children with bronchiolitis caused by respiratory syncytial virus (RSV)? *J. Clin. Nur.* 2: 2723-2733.

Katiyar-Agarwal S, Morgan R, Dahlbeck D, Borsani O, et al. (2006). A pathogen-inducible endogenous siRNA in plant immunity. *Proc. Natl. Acad. Sci. U. S. A.* 10: 18002-18007.

Lee J and Kim D-W (2012). Efficient multivariate feature filter using conditional mutual information. *Electron. Lett.* 4: 161-162.

Lipson RS, Webb KJ and Clarke SG (2010). Rmt1 catalyzes zinc-finger independent arginine methylation of ribosomal protein Rps2 *Saccharomyces cerevisie*. *Biochem. Biophys. Res. Comm.* 39: 1658-1662.

Lyczkowski D, Moschovis P and Qazi S (2014). Acute Respiratory Infections. In: The MassGeneral Hospital for Children Handbook of Pediatric Global Healt: (Gupta N, Nelson BD, Kasper J, and Hibberd PL, eds.) Springer, New York, 193-203.

Mailhammer R, Szöts H, Bönisch J and Dörmer P (1992). Downregulation of messenger RNA levels for ribosomal proteins in differentiating HL-60 cells. *Exp. Cell. Res.* 20: 145-148.

Malygin AA, Parakhnevitch NM, Ivanov AV, Eperon IC, et al. (2007). Human ribosomal protein S13 regulates expression of its own gene at the splicing step by a feedback mechanism. *Nucleic Acids Res.* 3: 6414-6423.

Mazumder B, Poddar D, Basu A, Kour R, et al. (2014). Extraribosomal l13a is a specific innate immune factor for antiviral defense. *J. Virol.* 88: 9100-9110.

Mejias A, Dimo B, Suarez NM, Garcia C, et al. (2013). Whole blood gene expression profiles to assess pathogenesis and disease severity in infants with respiratory syncytial virus infection. *PLoS Med.* 1: 12.

Meriin AB, Zaarur N and Sherman MY (2012). Association of translation factor eEF1A with defective ribosomal products generates a signal for aggresome formation. *J. Cell Sci.* 12: 2665-2674.

Provost E, Weier CA and Leach SD (2013). Multiple Ribosomal Proteins Are Expressed at High Levels in Developing Zebrafish Endoderm and Are Required for Normal Exocrine Pancreas Development. *Zebrafish* 1: 161-169.

Russo A, Esposito D, Catillo M, Pietropaolo C, et al. (2013). Human rpL3 induces G_1/S arrest or apoptosis by modulating p21(waf1/cip1) levels in a p53-independent manner. *Cell Cycle* 1: 76-87.

Smoot ME, Ono K, Ruscheinski J, Wang P-L, et al. (2011). Cytoscape 2.8: new features for data integration and network visualization. *Bioinformatics* 2: 431-432.

Smyth GK (2004). Linear models and empirical bayes methods for assessing differential expression in microarray experiments. *Stat. Appl. Genet. Mol. Biol.* 3.

Spinelli L, Gambette P, Chapple CE, Robisson B, et al. (2013). Clust&See: a Cytoscape plugin for the identification, visualization and manipulation of network clusters. *Biosystems* 11: 91-95.

Wang CC, Kadota M, Nishigaki R, Kazuki Y, et al. (2004). Molecular hierarchy in neurons differentiated from mouse ES cells containing a single human chromosome 21. *Biochem. Biophys. Res. Commun.* 31: 335-350.

Wasserman S and Faust K (1994). Social network analysis: Methods and applicatios: Cambridge university press, New York and Cambridge.

Zaas AK, Chen M, Varkey J, Veldman T, et al. (2009). Gene expression signatures diagnose influenza and other symptomatic respiratory viral infections in humans. *Cell Host Microbe* 3: 207-217.